Automated wire tension measurement system for LHCb muon chambers

P. Ciambrone[a], E. Dané[b], R. Dumps[c], M. Dwuznik[c,1], G. Felici[a], C. Forti[a], A. Frenkel[b], J.-S. Graulich[c], A. Kachtchouk[c], V.V. Kulikov[d], G. Martellotti[b], A. Medvedkov[b], A.A. Nedosekin[d], G. Penso[b,*], D. Pinci[b], G. Pirozzi[b], B. Schmidt[c], V. Shubin[e,2]

[a]*Laboratori Nazionali di Frascati, Frascati, Italy*
[b]*Università "La Sapienza" and INFN, Roma, Italy*
[c]*CERN, Genève, Switzerland*
[d]*Institute for Theoretical and Experimental Physics, Moscow, Russia*
[e]*Joint Institute for Nuclear Research, Dubna, Russia*

Abstract

A wire tension meter has been developed for the multi-wire proportional chambers of the LHCb muon detector. The wire tension is deduced from its mechanical resonance frequency. In the LHCb muon chambers, the wires are 2 mm apart and electrically connected in groups of 3–32, so that the wire excitation system must be precisely positioned with respect to the wire to be tested. This wire is forced to oscillate by a periodic high voltage applied between that wire and a non-oscillating "sense wire" placed parallel and close to it. This oscillation produces a variation of the capacitance between these two wires which is measured by a high precision digital electronic circuit. At the resonance frequency this capacitance variation is maximum. The system has been systematically investigated and its parameters were optimized. In the range 0.4–1 N a good agreement is found between the mechanical tension measured by this system and by a dynamometer.
© 2005 Elsevier B.V. All rights reserved.

---

*Corresponding author.
E-mail address:* gianni.penso@roma1.infn.it (G. Penso).
[1]Now at AGH University of Science and Technology, Cracow, Poland.
[2]Now at CERN, Genève, Switzerland.

1. Introduction

The LHCb experiment, one of the four experiments that will operate at the Large Hadron Collider (LHC) at CERN, is dedicated to the study of rare phenomena, and in particular the CP-violating decays of beauty hadrons. In many of these decays, muons are present in the final state so that muon triggering and offline muon identification are fundamental requirements of the experimental set-up. The muon detector [1] consists of five muon tracking stations placed along the beam axis. The first station (M1) is placed in front of the electromagnetic and hadronic calorimeters. The remaining four stations (M2–M5) are interleaved with three iron filters and placed downstream of the calorimeters. The five stations comprise more than 1300 multi-wire proportional chambers. The chambers contain two wire planes in M1 station and four wire planes in M2–M5 stations. Altogether the number of wire planes is $\sim$5000. A wire plane comprises about 150–740 wires, depending on its location in the five stations. The distance between two neighbouring wires is 2 mm. The total number of wires whose mechanical tension must be checked is $\sim$3.2 millions. In order to detect any possible failure occurring during the wiring process, the wire tension check must be performed online during the chamber production, so that a fast, automated and reliable system is needed. In the present paper we present a systematic study of the performance of the wire tension meter we have designed and realized for the multi-wire proportional chambers of the LHCb muon detector.

2. Principle of operation

The mechanical tension τ of a wire is deduced from the measurement of its fundamental mechanical resonance frequency v_0; these two quantities are related by the formula

$$\tau = \lambda(2\ell v_0)^2 \qquad (1)$$

where λ and ℓ are, respectively, the mass per unit length and the length of the wire. In the LHCb

chambers, wires are made[3] of gold-plated tungsten, 30 μm diameter, $\sim$20–32 cm long with a linear density $\lambda \simeq 13.6$ mg/m. Their tension should be in the range[4] 0.55–0.75 N which corresponds to a resonance frequency of $\sim$340–470 Hz, depending on the wire length.

Different methods have been adopted [2–9] to induce mechanical oscillations of the wire under test and to measure its resonance frequency. The wire tension measurement (WTM) system used for the LHCb muon chambers is based on the digital electrostatic method [5]. This method greatly improves the performances of a similar approach already proposed [9] with a limited success.

Mechanical oscillations of a chamber wire are induced by applying a periodic high voltage (HV) between a reference electrode (hereafter named ''sense wire''), close to the wire under test, and the chamber wire plane which is grounded. The resulting electrostatic force induces the chamber wire to oscillate. The resonance frequency v_0, is found as the value of the HV frequency (v) which maximizes the wire oscillation amplitude.

The oscillations of a chamber wire result in a periodical variation of the capacitance (C^*) between the chamber wire and the sense wire. The amplitude of this variation is measured by a digital system, as a function of v. The measurement of C^* is realized by coupling the capacitance C^* to the LC circuit of a high-frequency ($\approx$ 20 MHz) oscillator (Fig. 1). Considering that $C^* \ll C$ the oscillator frequency is:

$$f = \frac{1}{2\pi\sqrt{L[C + C^*]}} \simeq \frac{1}{2\pi\sqrt{LC}}\left(1 - \frac{C^*}{2C}\right). \qquad (2)$$

When the wire is oscillating at a frequency v, the capacitance C^* and therefore the high-frequency f varies periodically in time with a period $T = 1/v$. The amplitude Δf of the high-frequency variation is maximum at the resonance frequency v_0. To evaluate this amplitude, two values of f are measured at different phases with respect to the HV oscillation: $f_A(v, \phi_A)$ at a phase $\phi_A = 2\pi t/T = 2\pi vt$ (Fig. 2)

---

[3] by LUMA-METALL AB, Kalmar, Sweden; http://www.luma-metall.se.

[4] The wire tension is often improperly measured in grams, a gram being ''equivalent'' to 9.81 mN.
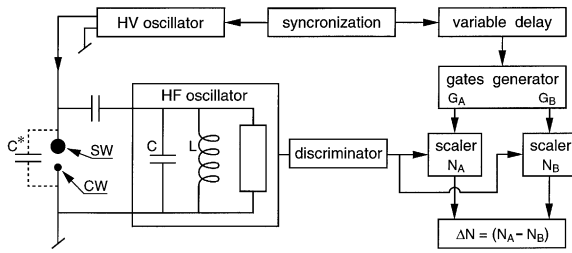
Fig. 1. Electronic scheme for measuring the variation of the capacitance (C^*) between the chamber wire (CW) and the sense wire (SW).
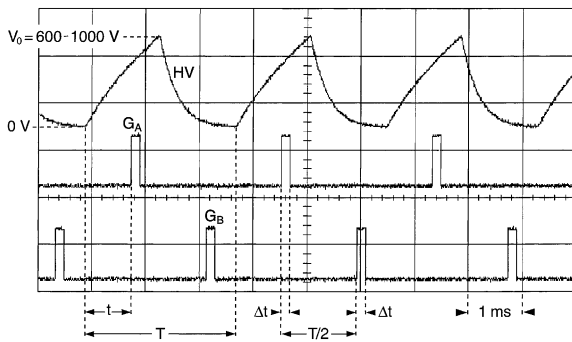

Fig. 2. Waveforms and timing of the high-voltage oscillator and of the gates G_A and G_B.

and $f_B(v, \phi_B)$ at a phase[5] $\phi_B = \phi_A + \pi$. By varying v and t (i.e. ϕ_A) we search for the maximum value of $\Delta f(v, \phi_A) = f_A(v, \phi_A) - f_B(v, \phi_B)$. This maximum occurs for $v = v_0$ and at a particular value of ϕ_A which is fixed once the HV waveform is settled.

The frequencies $f_A(v, \phi_A)$ and $f_B(v, \phi_B)$ are measured by counting the discriminated high-frequency oscillations during two identical phase intervals $\Delta\phi$ (corresponding to a time interval $\Delta t = T\Delta\phi/2\pi$) determined by the gates G_A and G_B (Figs. 1 and 2). The obtained countings are respectively $N_A = f_A \Delta t$, $N_B = f_B \Delta t$. Their difference $\Delta N = N_A - N_B = \Delta f \Delta t$ is large only around the resonance frequency v_0. This results in a very

good signal-to-noise ratio in the measurement of $\Delta N(v)$. Moreover N_A and N_B are measured at a relative time distance (equal to $T/2$) of the order of a millisecond, so that their difference ΔN is insensitive to an eventual long-term frequency instability of the high-frequency oscillator. To achieve a better precision, the countings can be repeated during many consecutive periods T, and then averaged.

3. The automated set-up

The set-up for wire tension measurements consists (Fig. 3) of a steady table of about $0.6 \times 2\,\mathrm{m}^2$, on which the chamber wire plane to be tested is fixed. To speed up the wire tension tests, 12 sense wires, parallel to the chamber wires, measure as many wires of a wire plane at the same time. The 12 sense wires are fixed to a carriage (Fig. 3) which can be moved perpendicularly to the chamber wires. The distance between two neighbouring sense wires is 12 mm, which is sufficiently large to avoid any interference between them. The sense wires are centred longitudinally on the chamber wires to be tested and their length is about $\frac{1}{2}$ of the chamber wire length, so that the chamber wire vibrates essentially at its fundamental frequency. The sense wires are 100 µm in diameter. Their mass per unit length and their tension are chosen in such a way that their resonance frequency is far (higher by a factor $\gtrsim 2$) from that of the chamber wires. Therefore, the sense wires can be considered as stationary in the explored range of frequency v.

The carriage, which supports the sense wires, can be moved horizontally by means of a precision worm screw (Fig. 3), driven by a stepper motor, type Phytron[6] ZSH 87/2.200.6. The movement is controlled by a stepper motion controller from National Instruments (NI)[7], type NI PCI-7334. This system allows the positioning of the carriage with a precision of about ±100 µm. The motion

---

[5]The choice of $\phi_B = \phi_A + \pi$ is justified by the observation (see next section) that $f(t)$ is, with very good approximation, a sinusoidal function, so that the phase difference between its maximum and minimum values is π radians.

[6]Phytron-Elektronic GmbH, D-82194 Gröbenzell, Germany; http://www.phytron.de/.

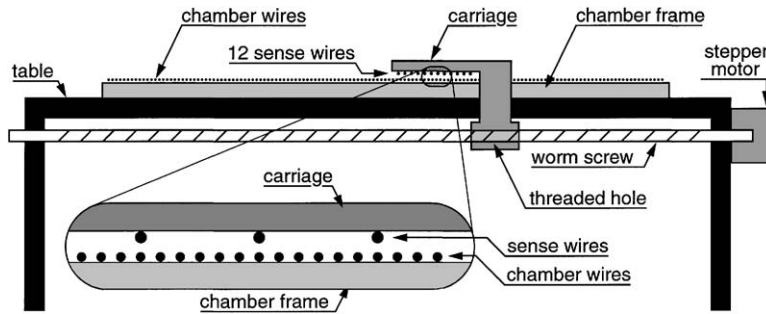[7]National Instruments Corp., Austin, TX 78759-3504, USA; http://www.ni.com/.

Fig. 3. Schematic view (not in scale) of the set-up. The chamber wire plane under test is fixed on the table. The 12 sense wires are fastened to the carriage which can be moved by means of a worm screw and a stepper motor. The position during the measurements of the sense wires with respect to the chamber wires is shown in the insert.

controller card is inserted in a computer operating under Windows XP. Two NI PCI-6602 cards are also inserted in that computer. All the NI cards are controlled by the NI LabVIEW software. The two NI PCI-6602 cards comprise 16 counter/timer modules: 12 of them are used as scalers to count the ΔN values (Fig. 1) relative to the 12 sense wires. The other modules generate the gate signals (Fig. 2), and a square wave signal having the wire excitation frequency v. This square wave signal drives a HV transistor, type TIPL 760A, mounted on the carriage and connected to the 12 sense wires. The amplitude (V_0, Fig. 2) of the signal delivered by the HV transistor is ~600–1000 V and its frequency (v) is varied in steps of 0.3–1 Hz in an interval of about ± 30 Hz around the frequency corresponding to the wire nominal tension.

The 12 HF oscillators (Fig. 1) are mounted on the carriage, close to their respective sense wires. The distance between the sense wires and the chamber wire plane can be regulated by acting on a special screw placed on the carriage. The adjustment of this distance is important because the chamber wires are electrically connected in group of ~3–32 (depending on the chamber location in the LHCb experiment). Therefore the HV applied to a sense wire excite mechanically not only the chamber wire in front of it but also the neighbouring chamber wires belonging to the same group. To avoid any interference from these neighbouring wires, the distance between the sense wires and the chamber wire plane must be lower than ~1.2 mm.

4. Results

In Fig. 4 we report the measured values of $\Delta N(v, \phi_A)$ performed on a single wire of a chamber wire plane. In these measurements Δt is equal to $T/20$ (corresponding to $\Delta \phi = \pi/10$), and ϕ_A is varied in step of $\pi/8$, so that the eight series of measurements reported in Fig. 4 refer to non-overlapping $\Delta \phi$ intervals. This phase scanning allows one to fix the best phase value for systematic measurements. In our case, the maximum value (ΔN_{max}) of $\Delta N(v, \phi_A)$ is obtained at a phase $\phi_A = \phi_0 \simeq \pi/4$ (Fig. 4c) and at the frequency $v = v_0 \simeq 377$ Hz ($\Delta N_{max} = \Delta N(v_0, \phi_0)$). For $\phi_A = \phi_0$ the resonance curve is symmetrical around the resonance frequency v_0, with a FWHM equal to ~1.2 Hz.

Mechanical and electronic noise may result in fluctuations on the measured ΔN values. In the data reported in Fig. 4 these fluctuations have been reduced by averaging 100 repeated measurements. This allows one to obtain clean resonance peaks on a smooth baseline, but increases the time needed to determine the tension of a wire. For a faster measurement, the number of averaged data can be reduced provided that the fluctuations remain small compared to ΔN_{max}, so as to avoid misidentification of the resonance peak. Alternatively, the measurements can also be sped up by increasing the gate length Δt up to a value in the interval $T/4 \leqslant \Delta t \leqslant T/2$, while keeping the gate centre at the same phase as in Fig. 4c: $\phi_{centre} = \phi_0 + \Delta \phi/2 \simeq 3\pi/10$.
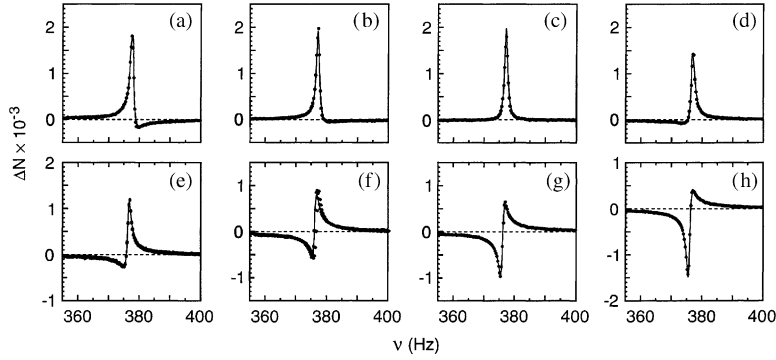
Fig. 4. Difference of the scalers' counting N_A and N_B (see Fig. 1) as a function of the wire excitation frequency v, for eight different values of ϕ_A: (a) $\phi_A = 0$, (b) $\phi_A = \pi/8$, (c) $\phi_A = \pi/4$, (d) $\phi_A = 3\pi/8$, (e) $\phi_A = \pi/2$, (f) $\phi_A = 5\pi/8$, (g) $\phi_A = 3\pi/4$, (h) $\phi_A = 7\pi/8$. All the measurements refer to a phase interval $\Delta\phi = \pi/10$ (see text). The lines are fits to the experimental points, with the Eq. (5). The same values of $\Delta N(v)$, but with an opposite sign, are obtained for $\phi_A \rightarrow \phi_A + \pi$.

The behaviour of $\Delta N(v, \phi_A)$ observed in Fig. 4 can be well described assuming that the chamber wire oscillates harmonically:

$$d(t) = d_0 + D(v)\cos\left(2\pi v t - \phi(v)\right) \qquad (3)$$

where $d(t)$ is the effective time-dependent distance[8] between the sense wire and the oscillating chamber wire and d_0 is the central value of $d(t)$. $D(v)$ and $\phi(v)$ are respectively the oscillation amplitude and its phase with respect to the HV excitation. In the approximation of parallel sense and chamber wires, the capacitance between these two wires is given, with a good approximation, by the formula:

$$C^*(t) = \frac{\pi\varepsilon_0 l}{\ln\left(d(t)/\sqrt{ab}\right)} \qquad (4)$$

where a and b are the two wire radii and l is the sense-wire length. By combining Eqs. (2), (3) and (4) we obtain

$$\Delta N = N_A(v, \phi_A) - N_B(v, \phi_A) \qquad (5)$$

where

$$N_A(v, \phi_A)$$
$$\propto 1/\sqrt{1 + \alpha_1/\ln[\alpha_2 + (D(v)/\sqrt{ab})\cos(\phi_A - \phi(v))]},$$
$$(6)$$

$$N_B(v, \phi_A)$$
$$\propto 1/\sqrt{1 + \alpha_1/\ln[\alpha_2 - (D(v)/\sqrt{ab})\cos(\phi_A - \phi(v))]},$$
$$(7)$$

$$D(v)/\sqrt{ab} = \alpha_3\alpha_4 v_0/\sqrt{(v^2 - v_0^2)^2 + (\alpha_4 v)^2}, \qquad (8)$$

$$\phi(v) = \tan^{-1}(\alpha_4 v/(v_0^2 - v^2)) \qquad (9)$$

and where α_1, α_2, α_3, α_4 and v_0 are the parameters of a fit to the experimental points of Fig. 4, obtained with Eqs. (5), (6), (7), (8) and (9). The agreement is quite good. It turns out from the fit that $\alpha_3/\alpha_2 = D(v_0)/d_0 \ll 1$, which is equivalent to the small-oscillation approximation. In that case the Eqs. (6) and (7) simplify and Eq. (5) becomes $\Delta N(v, \phi_A) = \beta(v)\cos(\phi_A - \phi)$, where $\beta(v)$ is a function of v. The dependence of $\Delta N(v, \phi_A)$ on ϕ_A has been measured at the resonance frequency v_0. The results are reported in Fig. 5 together with a sinusoidal fit to the experimental points. The nearly sinusoidal behaviour of $\Delta N(v_0, \phi_A)$ validates our assumption that the chamber-wire oscillates harmonically also for a non-sinusoidal HV excitation and indicates that the amplitude of the chamber-wire oscillations is small compared to the distance d_0 between the chamber-wire and the sense wire.

The dependence of ΔN_{max} on the high-voltage amplitude V_0 (Fig. 2) has been measured and the results are reported in Fig. 6. The experimental
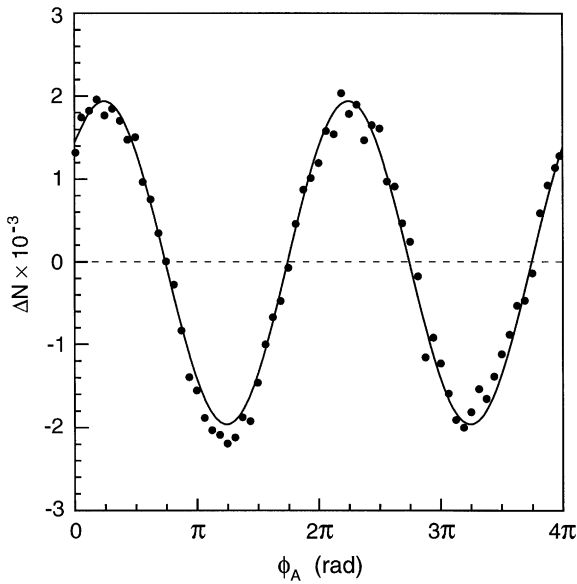
---

[8]During the oscillations, the chamber wire is no longer parallel to the sense wire. However this effect has been neglected and an effective distance between the two wires is defined as their distance averaged on their length.

Fig. 5. ΔN measured at the resonance frequency ν_0, as a function of the phase ϕ_A. The curve is a sinusoidal fit to the experimental points.

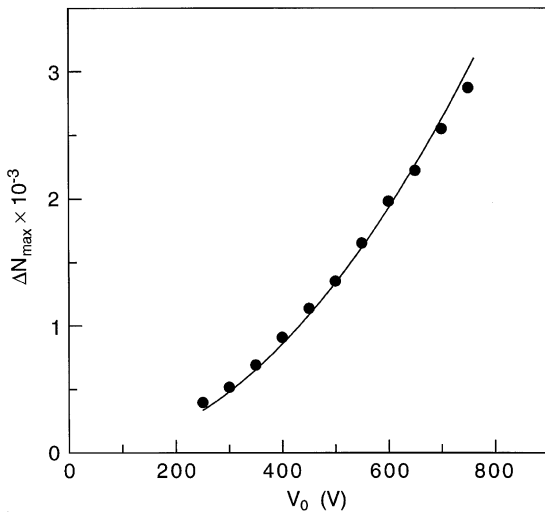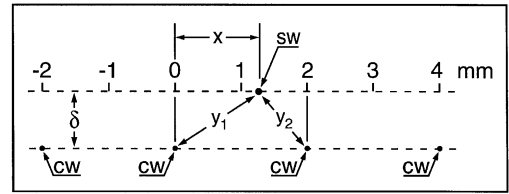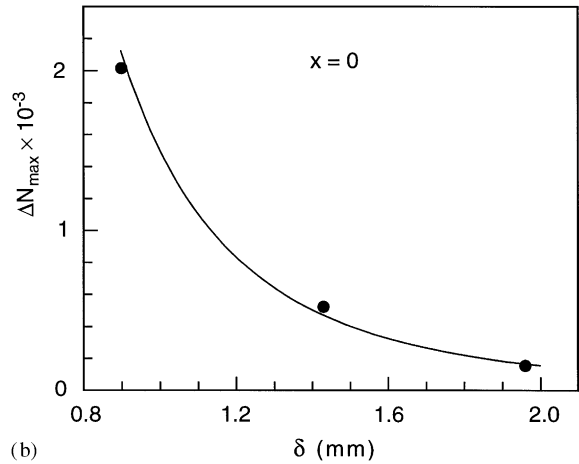Fig. 6. ΔN_{max} measured as a function of the excitation high-voltage amplitude V_0. The line is a fit to the experimental data with the expected law $\Delta N_{max} \propto V_0^2$.

data follow with good precision the expected[9] law $\Delta N_{max} \propto V_0^2$.

---

[9]For small oscillations ΔN_{max} is proportional to the amplitude of the driving force which in turn is proportional to V_0^2.

Fig. 7. (a) Position of the sense wire (SW) with respect to the chamber wires (CW) during the positioning tests. The origin of the x-axis is placed "in front" of an arbitrary chamber wire. During normal measurements $\delta \simeq 0.9$ mm and the sense wire is "in front" ($x = 0$) of the chamber wire to be measured. (b) ΔN_{max} measured at $x = 0$, as a function of the distance δ between the sense wire and the chamber wire plane. The line is a fit to experimental points with a power law $\Delta N_{max} \propto \delta^{-3.2}$.

In order to determine the precision required in the positioning of the sense wire with respect to the chamber wire to be tested, ΔN_{max} has been measured at different positions (x and δ, Fig. 7a) of the sense wire with respect to the chamber wires. In Fig. 7b we show the dependence of ΔN_{max} on the distance δ while keeping the sense wire "in front" ($x = 0$) of a chamber wire. A fit to the data with an empirical power law leads to $\Delta N_{max} \propto \delta^{-3.2}$. At a large distance ΔN_{max} may become comparable with the noise, therefore a distance δ lower than ~ 1.2 mm is recommended. A distance $\delta \simeq 0.9$ mm has been chosen for the systematic wire tension check of the produced chambers.

A second set of measurements of ΔN_{max} has been performed by fixing $\delta \simeq 0.9$ mm and by

varying the position of the sense wire between two neighbouring chamber wires ($0 < x < 2$ mm, Fig. 7a). In this geometrical situation the two chamber wires closer to the sense wire can be simultaneously excited, so both their oscillations can contribute to ΔN_{max}. In order to disentangle these two contributions, the sense wire was moved between two chamber wires having slightly different resonance frequencies v_1 and v_2. This results, for $0 < x < 2$ mm, in a double-peaked excitation curve as shown in Fig. 8a. In Fig. 8b the amplitudes of these two peaks are reported as a function of x. A fit to the experimental points is obtained with an empirical power law $\Delta N_{max} \propto y_{1,2}^{-5.1}$, where $y_{1,2}(x)$ are the distances between the sense wire and the two neighbouring chamber wire (Fig. 7a). The results reported in Fig. 8b show that a precision of about ± 200–300 μm in sense wire
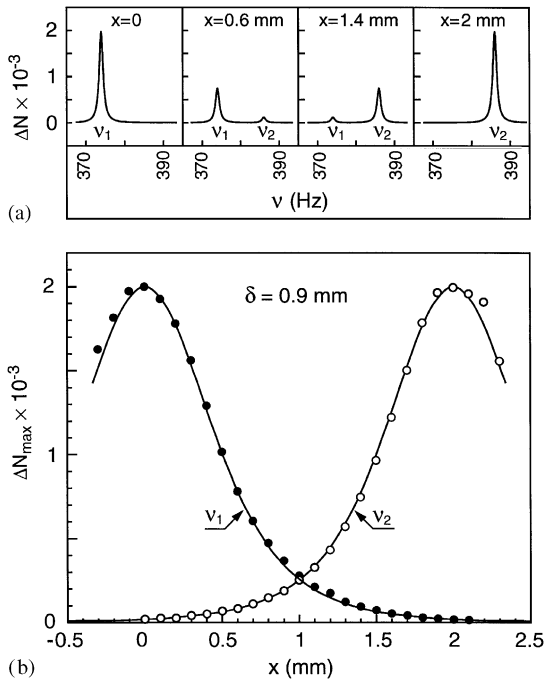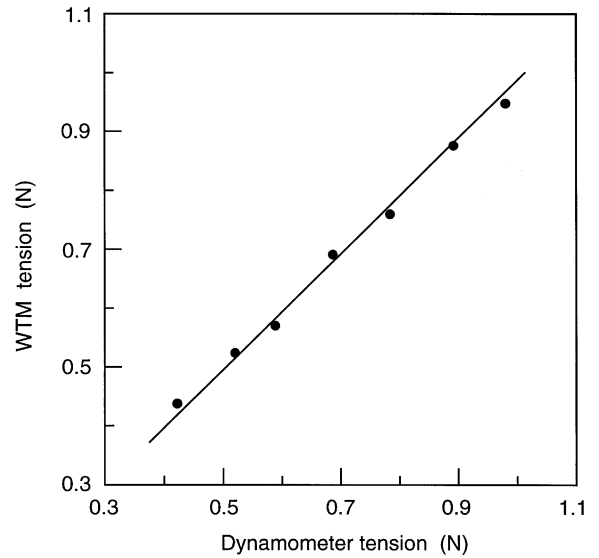

Fig. 9. Comparison of the tension of a wire measured by the present wire tension measurement (WTM) system and with a dynamometer. The line is a linear fit to the experimental points.

carriage positioning is sufficient to avoid an interference of the two neighbouring chamber wires.

In order to check the correct operation of the whole system, the tension of a wire was measured with a dynamometer and with the described set-up. The results, reported in Fig. 9, show that in the explored range 0.4–1.0 N, the automated wire tension measurement system has a linear response and provides, within a few percent, the correct tension values.

The position of the peaks, i.e. the resonance frequency v_0 of the wires under test is determined by a program[10] based on NI LabVIEW which runs on the same computer where NI cards are inserted. The full system with 12 sense wires allows one to measure the tension of about 1300 wires per hour; a rate sufficiently high to follow the chamber production rate. In Fig. 10 the result of an automated wire tension measurement performed on a 200 wire plane is shown. The tensions

(a)

(b)

Fig. 8. (a) Excitation curves obtained for four different x-positions of the sense wire. The distance δ was equal to 0.9 mm. The two peaks occur at the resonance frequencies of the two neighbouring chamber wires, $v_1 \simeq 374$ Hz and $v_2 \simeq 386$ Hz. (b) Amplitude of the resonance peaks occurring at the frequencies v_1 (full points) and v_2 (open points), as a function of the x-position of the sense wire. The lines are a fit to the experimental points (see text).

---

[10]For more details on resonance peak detection program see the LHCb-Muon-2004 Internal Notes: "WTM Program manual and description" and "Background detection and compensation in WTM peaks detection" by V. Shubin.
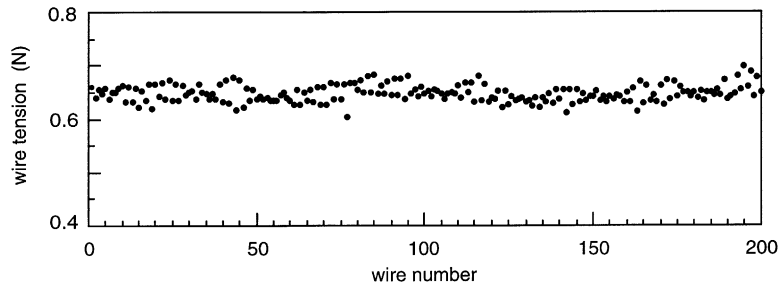
Fig. 10. Typical results of an automated wire tension measurement performed on a wire plane comprising 200 wires.

are distributed around 0.65 N with a spread of $\sim \pm 6\%$ in agreement with the design requirements.

5. Conclusions

An automated digital system for measuring the wire tension of the LHCb muon chambers has been developed and tested. The tension of a wire is deduced from the measurement of its mechanical resonance frequency. The forced wire oscillations are induced by a periodic high voltage applied between the wire under test and a sense wire parallel and close to it. The particular structure of the LHCb muon chamber wire planes (group of wires electrically connected with a distance of 2 mm between two neighbouring wires) makes a precise positioning (of few hundreds of microns) of the sense wire with respect to the chamber wire necessary. This is achieved by a servomechanism driven by a computer which also controls the digital electronics and carries out the data-taking

and analysis. The wire tension is determined with a precision of the order of 1%. The full system comprises 12 sense wires which measure at the same time 12 wires of a wire plane. This allows to measure the tension of about 1300 wires per hour. This rate is sufficient to check the wire tension of the muon chambers as they are produced.

References

[1] LHCb Collaboration, LHCb Muon System Technical Design Report, CERN/LHCC 2001-010 (2001); Addendum to the Muon System Technical Design Report, CERN/LHCC 2003-002 (2003).
[2] R. Stephenson, J.E. Bateman, Nucl. Instr. and Meth. 171 (1980) 338.
[3] M. Calvetti, et al., Nucl. Instr. and Meth. 174 (1980) 285.
[4] B. Brinkley, et al., Nucl. Instr. and Meth. A 373 (1996) 23.
[5] A. Andryakov, et al., Nucl. Instr. and Meth. A 409 (1998) 63.
[6] T. Ohama, et al., Nucl. Instr. and Meth. A 410 (1998) 175.
[7] A. Balla, et al., CERN/ATL-MUON-2000-002.
[8] B. Maréchal, et al., CERN/LHCb-MUON 2002-023.
[9] L.S. Durkin, et al., IEEE Trans. Nucl. Sci. NS-42 (1995) 1419.